AJNR

Phased-array surface coil MR of the orbits and optic nerves.

J Breslau, R W Dalley, J S Tsuruda, C E Hayes and K R Maravilla

This information is current as of April 19, 2024.

Phased-Array Surface Coil MR of the Orbits and Optic Nerves

Jonathan Breslau, Robert W. Dalley, Jay S. Tsuruda, Cecil E. Hayes, and Kenneth R. Maravilla

PURPOSE: To devise a practical technique for high-resolution evaluation of the anterior optic apparatus using a phased-array surface coil system, and to evaluate this system in patients with suspected optic pathway abnormalities. **METHODS:** A four-element phased-array coil pair was placed on each side of the head, and signal-to-noise measurements were obtained using a head phantom. Comparison between the phased-array coil, the quadrature coil, and a single-turn 12.7-cm (5-in) surface coil was done. T1 spin-echo and T2 fast spin-echo sequences were obtained in the oblique axial and oblique sagittal planes, to approximate the long axis of the optic nerves and the nonoblique coronal plane. **RESULTS:** The phantom signal-to-noise measurements at simulated locations of the optic nerve head, optic canal, and optic chiasm revealed an improvement of at least 30% using the phased-array system. Of 24 imaged cases, 9 had trauma, 5 had suspected neoplasms, and 2 had optic neuritis. In 3 patients, an unexpected diagnosis of optic pathway contusion or infarction was made. The remaining 8 patients had various suspected visual pathway lesions. **CONCLUSION:** Phased-array surface coils allow rapid, thin-section imaging of the entire anterior optic pathway, with improved signal-to-noise ratio. This may improve evaluation of optic pathway lesions over conventional techniques.

Index terms: Orbits, magnetic resonance; Nerves, optic (II); Magnetic resonance, technique

Magnetic resonance imaging of the optic pathway with high anatomic detail and contrast resolution presents a unique challenge. Images of this region may be degraded by ocular motion. Abundant orbital fat may hinder visibility of the optic nerve and other retrobulbar lesions. Currently, optimal imaging of the anterior optic pathway, which consists of the globes, optic nerves, optic chiasm, and optic tracts, requires both surface and conventional head coils.

Attempts to optimize orbital imaging have addressed these difficulties. Short scanning times minimize motion. Several methods have been developed to suppress the fat signal, often in conjunction with gadopentetate dimeglumine (1–3). However, the conflict between the superior signal-to-noise ratio of orbital surface coils and the large field of view of conventional head coils requires a compromise and remains a problem. The optimal system would possess an adequate signal-to-noise ratio to allow a minimum section thickness through the desired anatomy without increasing the number of excitations, yet maintain adequate penetration to image posterior to the orbital apex.

Previous studies have demonstrated that phased-array surface coil assemblies provide superior imaging of the pelvis (4), orbits (Gass A, "High Resolution Magnetic Resonance Imaging of the Anterior Visual Pathway Using Fast Spin Echo and Phased Array Local Coils," presented at the 12th Annual Scientific Meeting of the Society for Magnetic Resonance in Medicine, New York, NY, 1993), and, most recently, the temporal lobes (5). The purpose of this study was to apply this technology to image the anterior optic pathways and to determine whether significantly improved image quality can be obtained.
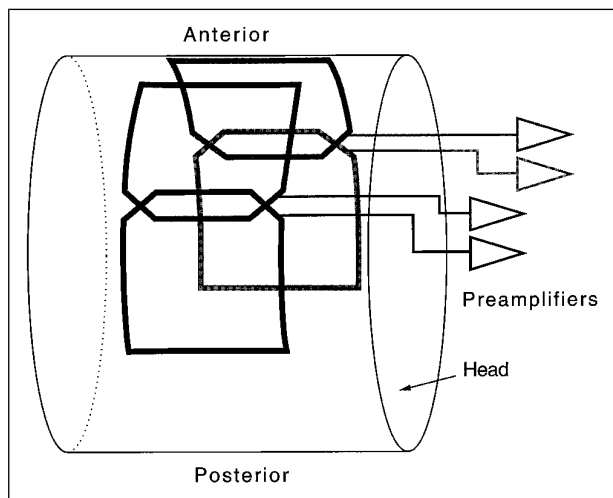
Fig 1. Water-filled head phantom with coil pairs placed for signal-to-noise measurement. This positioning also approximates their use in clinical studies.
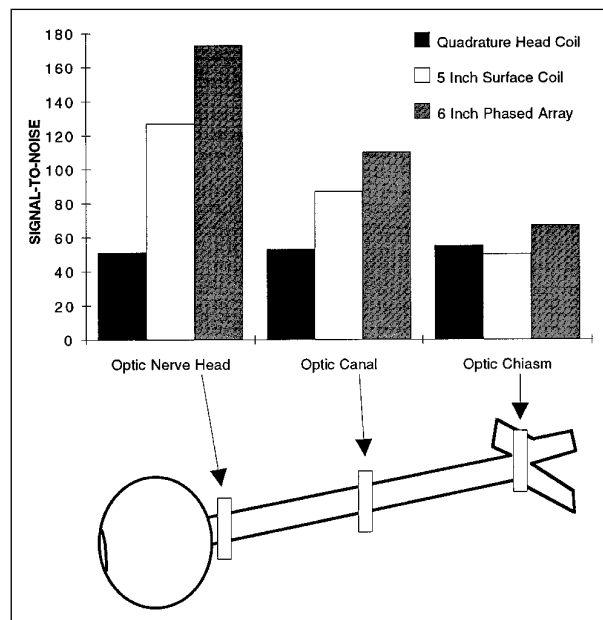

Fig 2. Calculated signal-to-noise ratio, averaged over six axial images, at estimated locations of the optic nerve head, optic canal, and optic chiasm. Measurements were made on the head phantom, using the quadrature head coil, the 5-in surface coil, and the phased-array system.

Methods

Design of the phased array has been previously described (5). Briefly, the system we used consisted of a phased-array coil pair. Each of the two individual coils was shaped to approximate the curve of the head, and each contained two overlapping elements measuring 16.5×10 cm. To obtain a quantitative measurement of the signal-to-noise ratio, we imaged a water-filled phantom, constructed to mimic the shape and tissue signal losses of the head. Because the phantom did not adequately load the quadrature head coil, a coil loader consisting of a resistive bird cage was placed around the phantom (5). Our signal-to-noise measurement procedure used 20×20-pixel squares averaged over six axial images at the estimated locations of the optic nerve head, optic canal, and the optic chiasm. To measure the signal-to-noise ratio for a phased array, both signal and noise must be acquired from the same region of interest within the image. We used the signal-to-noise calculation for a phased array that has been previously described by Hayes et al (6). Measurements of the phantom were also obtained with the quadrature head coil and the 5-in surface coil.

Imaging of patients was done with a 1.5-T magnetic resonance system (General Electric Medical Systems, Milwaukee, Wis). Phased-array coil pairs were placed obliquely over the orbits, on either side of the head, with approximately 4 cm of separation between the anterior edges of the coils (Fig 1) and 2 cm of distance between the coils and the surface of the eyelid. Subjects were instructed to keep their eyes open and fixed in a midline position.

Imaging protocol consisted of T1-weighted (600/16/2 [repetition time/echo time/excitations]) axial and sagittal and T2-weighted fast spin-echo (3850/92 effective/2) axial and coronal sequences. Oblique axial and sagittal planes were individually selected to approximate the long axis of the optic nerves. A coronal plane perpendicular to the horizontal plane of the optic nerves was also selected.

This view was important in separating partial volume artifacts from true abnormalities. Fat suppression was applied using a frequency-selective chemical shift presaturation pulse in all T2-weighted fast spin-echo sequences and in posttrauma T1-weighted sequences. In patients with suspected demyelination or neoplasms, post–gadopentetate dimeglumine T1-weighted images with fat suppression were also obtained in at least two planes. When imaging time allowed, additional sequences using a 512×256 matrix were also obtained and compared to the 256×256 matrix images. In the first patient imaged, axial and coronal short-tau inversion recovery (STIR) sequences were added. These were not used in other patients because of time limitations. Section thickness was 3 mm with a 1-mm intersection gap and a 14- or 16-cm field of view.

Imaging was initially performed on five healthy volunteers to assess the technical capacity of this new technique. Patients studied with this technique consisted of only those in whom there was a clinical need for precise delineation of a possible optic pathway lesion, determined after consultation with the referring clinician. We studied 26 patients with ages from 11 to 62 years. In 2 patients the images were not of diagnostic quality because of motion artifacts. Of the 24 remaining patients, 9 were imaged after trauma, 5 had suspected neoplasms, and 2 had a clinical picture of optic neuritis. The remaining 8 patients had a variety of lesions affecting the visual system. In the assessment of traumatic lesions in severely injured, intubated patients, imaging was performed after administration of a neuromuscular blocking agent, pancuronium.
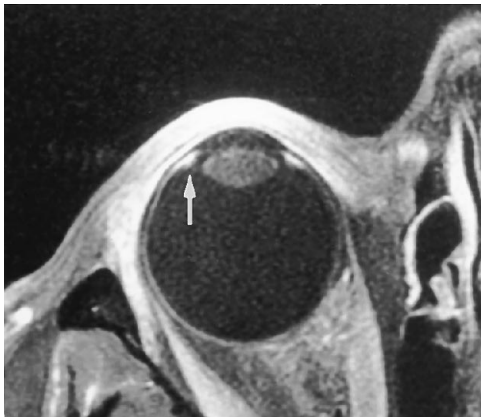
Fig 3. Ocular anatomy. Fat-suppressed T1-weighted (600/15) axial images after gadopentetate dimeglumine show the anatomy of the uveal tract, including the ciliary body (*arrow*) and the lens.

Results

Figure 2 displays the signal-to-noise ratio of the head coil, the anteriorly positioned 5-in surface coil, and the phased array at relevant locations along the optic pathway. Each value represents the average signal-to-noise ratio on six images of the same axial section. At all selected locations, the calculated signal-to-noise ratio of the phased array surpassed both the head coil and the selected surface coil by approximately 25% or greater.

Initial imaging studies on healthy volunteers were accomplished in approximately 40 minutes. These images clearly depicted normal ocular anatomy, including layers of the lens and components of the uveal tract (Fig 3). The entire course of the optic nerves, including the intracanalicular portion, and the chiasm were also displayed on a single imaging sequence.

The signal-to-noise ratio remained superior to the head coil as far posteriorly as the anterior optic tracts. We detected a qualitative loss of the signal-to-noise ratio using a 512 × 256 matrix (compare Fig 4A and B). These subjects did not experience any discomfort or heating during imaging.

Patients with traumatic optic neuropathy were potential candidates for surgical decompression of the optic canal. It was therefore important to distinguish between optic nerve contusion, compression, and transection, particularly in the intracanalicular portion (7, 8). Imaging was improved by the administration of pancuronium to intubated patients; the paralysis eliminated motion artifacts. The following were illustrative examples.

Patient 1 (Fig 4B) is a 22-year-old man who sustained extensive facial fractures after a motor vehicle accident. Eye examination was consistent with bilateral traumatic optic neuropathy. Coronal T2 fast spin-echo images showed a horizontal, ovoid area of T2 hyperintensity in the optic chiasm, interpreted as contusion. A similarly located coronal image including the optic chiasm of a healthy volunteer is shown for comparison (Fig 4A).

Patient 2 received a self-inflicted gunshot wound; the bullet entered in the right temple, coursed under the right optic nerve, and exited through the left orbit. Coronal T2-weighted fast spin-echo magnetic resonance images (Fig 5) demonstrate high signal in a short segment of the intraorbital optic nerve, thought to represent contusion from the shock wave of the passing bullet. This finding was also present in axial images.
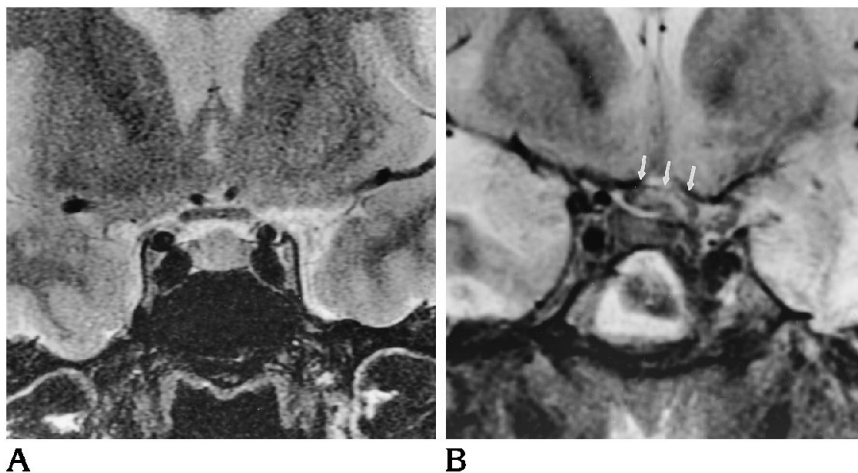

A   B

Fig 4. Healthy volunteer and chiasmatic contusion. *A*, T2-weighted (3100/92 effective) coronal image showing the chiasm of a healthy subject. This image was obtained with a 512 × 256 matrix. Note the signal-to-noise loss compared with *B*. *B*, T2-weighted (3100/92 effective) coronal image displays a swollen chiasm with internal ovoid high signal thought to represent contusion (*arrows*). Bilateral temporal and inferior frontal contusions are also present.
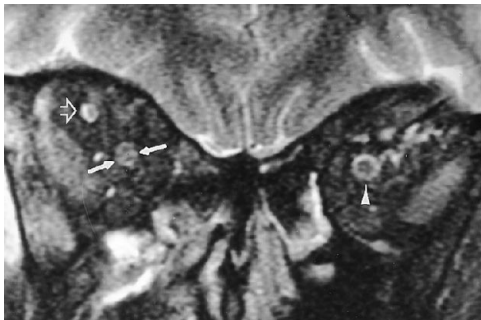
Fig 5. Right optic nerve contusion. T2-weighted (3500/96 effective) coronal image with fat suppression shows linear high signal in the right optic nerve (*between arrows*). Note the normal target appearance of the contralateral optic nerve (*arrowhead*) and the normal right superior ophthalmic vein (*open arrow*).

Patient 3 has multiple sclerosis and has had long-standing right optic neuritis. The visual pathway images, including STIR, clearly show bright signal in the right optic nerve (Fig 6A and B).

Finally, patient 4 has biopsy-proved sarcoidosis and experienced progressive loss of vision over a 4- to 6-month period. T1-weighted images after gadolinium administration show intense enhancement of both optic nerves (Fig 7). Additional images (not included) showed involvement of the entire optic chiasm and anterior optic tracts. Of note is the precision with which the bony optic canal can be seen.

Review of treatments after imaging revealed that in three of the nine patients who had trauma, optic nerve injury was excluded with increased confidence, and surgical decompressions were not performed.

Discussion

This phased-array coil system has been shown to have a higher signal-to-noise ratio than conventional head coils at locations as deep as the hippocampi. In fact, even at the midsagittal plane, where the chiasm would be located, the signal-to-noise ratio is about 20% higher than with the head coil (5). We have shown that this phased-array system, initially developed for imaging the temporal lobes, provides superior images of the anterior optic pathway. Our phantom study indicates that, with the exception of the optic chiasm location, the array adds at least 30% in signal-to-noise ratio at sampled regions, a difference almost equivalent to doubling the number of excitations. With our system, imaging can be accomplished within 40 minutes. Although we initially used a 512 × 256 matrix, which sometimes suffered from reduced signal, most of the imaging was performed with a 256 × 256 matrix, which improved signal-to-noise ratio. We did not measure the signal-to-noise ratio with a pair of 3-in surface coils, because they were not available. These coils would be expected to have improved the signal-to-noise ratio of the globes and anterior optic nerves but poorer penetration at the orbital apex than even the 5-in coil.

Using the phased array, we observed areas of suboptimal fat suppression along the margins of the sinuses anteriorly. We think this problem may be caused by bulk susceptibility, as observed with conventional head coil images, but it appears more prominent close to the phased-array coils, where the signal-to-noise ratio is very high. It is also possible that the array introduced inhomogeneities in the main magnetic field, B_0.

In addition to the phased-array coil, modifications in the imaging protocol were helpful for particular clinical situations. In patients with traumatic lesions, fat suppression was used on noncontrast T1-weighted images to improve detection of T1 shortening caused by hemorrhage. Oblique sagittal images oriented along the course of the optic nerves were important to exclude small contusions of the nerve or compression in the optic canal region. We were thus

Fig 6. Optic neuritis in a patient with multiple sclerosis. *A*, Oblique axial fast STIR (3000/34/160) image shows high signal intensity in the right optic nerve (*arrows*). *B*, Coronal fast STIR (3000/34/160) image also shows bright signal in the involved optic nerve (*arrow*) and the normal-appearing left optic nerve (*arrowhead*).
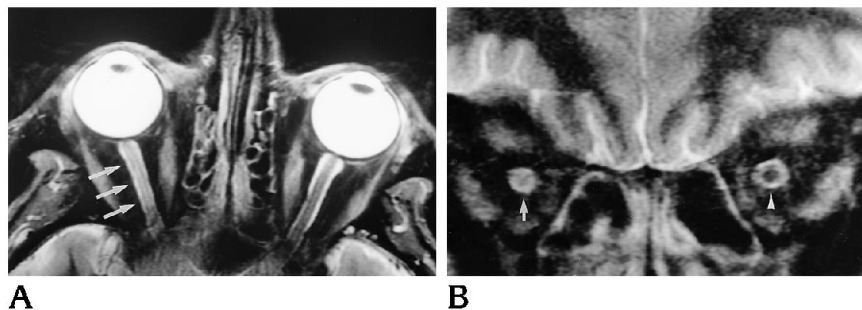

A

B

Fig 7. Patient with progressive loss of vision in both eyes and proved sarcoidosis involving lung, skin, and conjunctiva. Oblique axial (600/15) image after gadopentetate dimeglumine infusion show homogeneous intense enhancement of both optic nerves. Note the precise visibility of the cortical bone forming the optic canal on this imaging plane (*open arrows*).

able to locate lesions that would not be treated surgically, such as intraorbital optic nerve contusion, and exclude injury to the optic nerve with a high degree of confidence in patients with unexplained traumatic optic neuropathy.

In patients with suspected neoplastic or demyelinating lesions, fat suppression was used with the post–gadopentetate dimeglumine images and T2-weighted fast spin-echo images (9, 10). Coronal T2-weighted fast spin-echo images were important on all patients to confirm findings seen on sagittal or axial images.

In summary, we think that our phased-array system represents a major improvement for primary imaging of the anterior optic pathway. Because of the superior signal-to-noise ratio, thin sections can be obtained with only two excitations, which allows us to minimize imaging time. Our recommended protocol consists of T1- and T2-weighted oblique axial images along the plane of the optic nerves, oblique sagittal T1-weighted images also along the plane of the optic nerves, and nonoblique coronal T2-weighted images. If gadopentetate dimeglumine is administered, fat suppression is used for the axial and coronal T1-weighted images. In the setting of trauma, fat suppression is used on all noncontrast sequences. In patients investigated for possible optic neuritis, T2 fast spin-echo oblique sagittal imaging is obtained.

Acknowledgment

References

1. Tien R, Hesselink J, Szumowski J. MR fat suppression combined with Gd-DTPA enhancement in optic neuritis and perineuritis. *J Comput Assist Tomogr* 1991;15:223–227
2. Simon J, Szumowski J, Totterman S, et al. Fat-suppression imaging of the orbit. *AJNR Am J Neuroradiol* 1988;9:961–968
3. Hendrix L, Kneeland J, Haughton V, et al. MR imaging of optic nerve lesions: value of gadopentetate dimeglumine and fat-suppression technique. *AJNR Am J Neuroradiol* 1990;11:749–754
4. Hayes C, Dietz M, King B, Ehman R. Pelvic imaging with phased-array coils: quantitative assessment of signal-to-noise ratio improvement. *J Magn Reson Imaging* 1992;2:321–326
5. Hayes C, Tsuruda J, Mathis C. Temporal lobes: surface MR coil phased-array imaging. *Radiology* 1993;189:918–920
6. Hayes C, Hattes N, Roemer P. Volume imaging with MR phased arrays. *Magn Reson Med* 1991;18:309–319
7. Domingo Z, De Villiers J. Post-traumatic chiasmatic disruption. *Br J Neurosurg* 1993;7:141–148
8. Mark A, Phister S, Jackson D, Kolsky M. Traumatic lesions of the suprasellar region: MR imaging. *Radiology* 1992;182:49–52
9. Guy J, Mao J, Bidgood W, Mancuso A, Quisling R. Enhancement and demyelination of the intraorbital optic nerve. *Ophthalmology* 1992;99:713–719
10. Miller D, MacManus D, Bartlett P, Kapoor R, Morrissey S, Moseley I. Detection of optic nerve lesions in optic neuritis using frequency-selective fat-saturation sequences. *Neuroradiology* 1993;35:156–158